Novel nanocomposites from spider silk-silica fusion (chimeric) proteins

Cheryl Wong Po Foo, Siddharth V. Patwardhan, David J. Belton, Brandon Kitchel, Daphne Anastasiades, Jia Huang, Rajesh R. Naik, Carole C. Perry, and David L. Kaplan

PNAS published online Jun 12, 2006;
doi:10.1073/pnas.0601096103

Novel nanocomposites from spider silk–silica fusion (chimeric) proteins

Cheryl Wong Po Foo*, Siddharth V. Patwardhan†, David J. Belton†, Brandon Kitchel*, Daphne Anastasiades*, Jia Huang*, Rajesh R. Naik‡, Carole C. Perry†§, and David L. Kaplan*¶

*Departments of Biomedical Engineering, Chemistry, and Chemical and Biological Engineering, Bioengineering and Biotechnology Center, Tufts University, Medford, MA 02155; †Biomolecular and Materials Interface Research Group, School of Biomedical and Natural Sciences, Nottingham Trent University, Nottingham NG11 8NS, United Kingdom; and ‡Materials and Manufacturing Directorate, Air Force Research Laboratory, 3005 Hobson Way, Wright–Patterson Air Force Base, OH 45433-7702

Edited by Charles R. Cantor, Sequenom, Inc., San Diego, CA, and approved May 8, 2006 (received for review February 10, 2006)

Silica skeletal architectures in diatoms are characterized by remarkable morphological and nanostructural details. Silk proteins from spiders and silkworms form strong and intricate self-assembling fibrous biomaterials in nature. We combined the features of silk with biosilica through the design, synthesis, and characterization of a novel family of chimeric proteins for subsequent use in model materials forming reactions. The domains from the major ampullate spidroin 1 (MaSp1) protein of *Nephila clavipes* spider dragline silk provide control over structural and morphological details because it can be self-assembled through diverse processing methods including film casting and fiber electrospinning. Biosilica nanostructures in diatoms are formed in aqueous ambient conditions at neutral pH and low temperatures. The R5 peptide derived from the silaffin protein of *Cylindrotheca fusiformis* induces and regulates silica precipitation in the chimeric protein designs under similar ambient conditions. Whereas mineralization reactions performed in the presence of R5 peptide alone form silica particles with a size distribution of 0.5–10 μm in diameter, reactions performed in the presence of the new fusion proteins generate nanocomposite materials containing silica particles with a narrower size distribution of 0.5–2 μm in diameter. Furthermore, we demonstrate that composite morphology and structure could be regulated by controlling processing conditions to produce films and fibers. These results suggest that the chimeric protein provides new options for processing and control over silica particle sizes, important benefits for biomedical and specialty materials, particularly in light of the all aqueous processing and the nanocomposite features of these new materials.

biomaterials | nanostructures | silaffin | biomineralization | ceramics

Complex mineralized composite systems in nature provide rich ground for insight into mechanisms of biomineralization and novel materials designs (1–4). Some of the more common sources of inspiration include seashells, insect exoskeletons, extracellular matrices involved in bone and other hard tissues, and biosilica skeletons. The formation of natural inorganic–organic composites is a multistep process, including the assembly of the extracellular matrix, the selective transportation of inorganic ions to discrete organized compartments with subsequent mineral nucleation, and growth delineated by preorganized cellular compartments. Silica skeletons found in nature are based on nanoscale composites wherein the organic components, usually proteins, are functional parts of the skeletal structures while also serving as silica-forming components (5, 6). As a result, materials' toughness is improved, strength is retained, and fine morphological control is achieved, all hallmark attributes of biological composites.

Silica is widespread in biological systems and serves different functions, including support and protection in single-celled organisms, such as diatoms through to higher plants and animals (7, 8). The remarkable morphological control *in vivo* that generates intricate patterns at small-length scales is species-specific and has attracted a great deal of interest in recent years because such features exceed the capabilities of present-day synthetic and technological approaches to materials engineering *in vitro*. In nature, the biosynthesis of biosilica from "silicon" *in vivo* occurs under mild ambient physiological conditions, around neutral pH and low temperatures of ≈4–40°C, and is facilitated by various biomolecules (5, 6, 9). Such conditions are in stark contrast to geochemical and industrial syntheses of silica *in vitro*, typically accomplished under much harsher conditions of higher temperatures and extremes of pH. The controlled formation of bioinspired silica structures with a range of proteins, peptides, and synthetic additives under various physical reaction environments has been reported (10). Various proteins have been isolated from biosilicas, in particular, siliceous frustules of a few selected diatoms of which some low-molecular-weight proteins, known as silaffins, and some even lower molecular weight compounds, termed polyamines, have also been suggested to play a crucial role in silica formation (11). *In vitro* studies of silica formation have also been performed by using synthetic variants of the R5 peptide that derives from the repeating motif found in silaffin proteins (11–16). Even though the lysine and serine groups are not posttranslationally modified in R5 peptide (unlike natural silaffins), this 19-aa unit is found to promote and regulate silica formation at neutral pH (under conditions that would not have been expected to generate silica). Specifically, the R5 peptide has been used to obtain spherical silica nanostructures by using various precursors (12, 14, 15) as well as structures with different morphologies, including arch shapes and elongated fibers (13).

In the present article we describe a novel biomimetic nanocomposite approach to synthesize silica composites using fusion (chimeric) proteins. Fusion proteins have found applications in a wide spectrum of areas such as the biomedical field [including immunology, cancer research, and drug delivery (17–20)] and materials science [self-assembled materials (e.g., gels), quantum dot bioconjugates, sensors, and inorganic materials synthesis (21–27)]. Here we describe new silica-based nanocomposites formed from bioengineered fusion proteins that consist of two components (Fig. 1*A*), and we propose a model for silk protein assembly into films and fibers and silica deposition onto the materials during the mineralization reactions (Fig. 1*B*). One part of the fusion protein is the R5 peptide, known for precipitating silica as previously described. The second part of the fusion protein is a self-assembling domain based

Conflict of interest statement: No conflicts declared.

This paper was submitted directly (Track II) to the PNAS office.

Freely available online through the PNAS open access option.

Abbreviation: SEM, scanning electron microscopy.

§To whom correspondence may be addressed at: Interdisciplinary Biomedical Research Centre, School of Biomedical and Natural Sciences, Nottingham Trent University, Clifton Lane, Nottingham NG11 8NS, United Kingdom. E-mail: carole.perry@ntu.ac.uk.

¶To whom correspondence may be addressed at: Department of Biomedical Engineering, Bioengineering and Biotechnology Center, Tufts University, 4 Colby Street, Medford, MA 02155. E-mail: david.kaplan@tufts.edu.

 www.pnas.org/cgi/doi/10.1073/pnas.0601096103

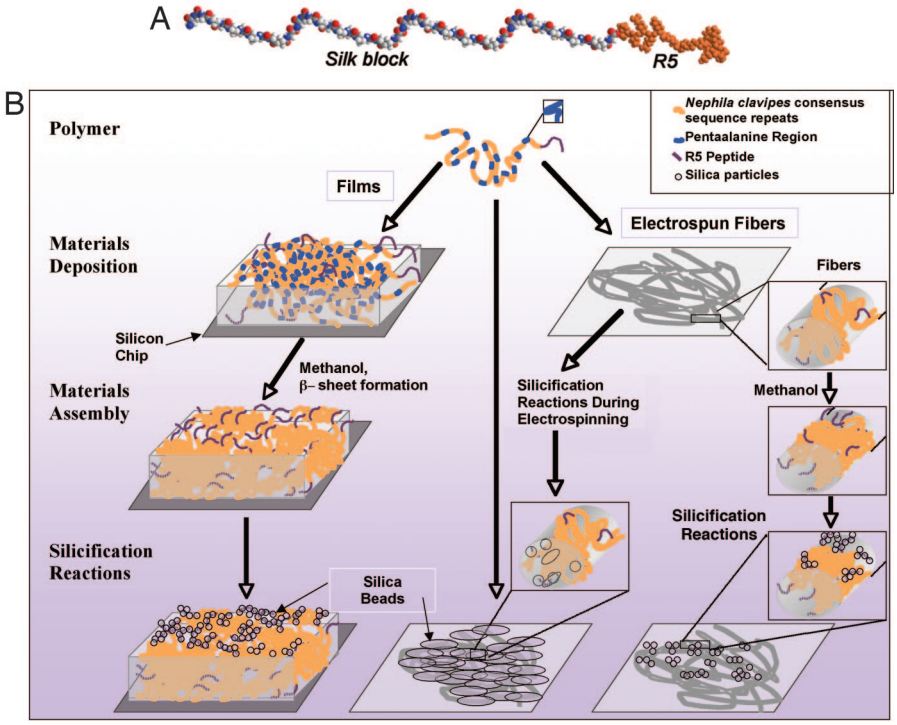

Fig. 1. Schematic representation of the design of fusion proteins and their use in controlled silica nanocomposite formation. (*A*) Scheme of chimeric design with two functional domains: silk and R5. (*B*) Model of spider silk protein processing into films and fibers and silicification reactions on the assembled materials.

on the consensus repeat in the major ampullate spidroin protein 1 (MaSp1) protein of *Nephila clavipes* spider dragline silk, known for the formation of highly stable (β-sheet) secondary structures with impressive mechanical properties. Importantly, in these designs we exploit two critical lessons in materials science and engineering from nature: (*i*) nanoscale structural protein materials are used to optimize mechanical function and materials stability, and (*ii*) improved materials properties are gained through the control of nanoscale organic–inorganic interfaces and composite structural features.

Silks are intriguing biologically derived proteins that form into fibers with remarkable mechanical properties (28, 29). In addition, silks self-assemble readily into defined β-sheet structures. Peptide variants of silkworm fibroin silk and spider dragline silks, as well as native reprocessed and genetic variants of these silks, have been studied to elucidate the important sequence chemistry–assembly

A **CRGD15mer+R5**

```
MASMTGGQQM GRGSCRGDTS GRGGLGGQGA GAAAAAGGAG QGGYGGLGSQ GTSGRGGLGG   60
QGAGAAAAAG GAGQGGYGGL GSQGTSGRGG LGGQGAGAAA AAGGAGQGGY GGLGSQGTSG  120
RGGLGGQGAG AAAAAGGAGQ GGYGGLGSQG TSGRGGLGGQ GAGAAAAAGG AGQGGYGGLG  180
SQGTSGRGGL GGQGAGAAAA AGGAGQGGYG GLGSQGTSGR GGLGGQGAGA AAAAGGAGQG  240
GYGGLGSQGT SGRGGLGGQG AGAAAAAGGA GQGGYGGLGS QGTSGRGGLG GQGAGAAAAA  300
GGAGQGGYGG LGSQGTSGRG GLGGQGAGAA AAAGGAGQGG YGGLGSQGTS GRGGLGGQGA  360
GAAAAAGGAG QGGYGGLGSQ GTSGRGGLGG QGAGAAAAAG GAGQGGYGGL GSQGTSGRGG  420
LGGQGAGAAA AAGGAGQGGY GGLGSQGTSG RGGLGGQGAG AAAAAGGAGQ GGYGGLGSQG  480
TSGRGGLGGQ GAGAAAAAGG AGQGGYGGLG SQGTSRGDCG SEFSSKKSGS YSGSKGSKRR  540
ILCGRHHHHH H                                                       551
```

B **15mer+R5**

```
MHHHHHHSSG LVPRGSGMKE TAAAKFERQH MDSPDLGTDD DDKAMASGRG GLGGQGAGAA   60
AAAGGAGQGG YGGLGSQGTS GRGGLGGQGA GAAAAAGGAG QGGYGGLGSQ GTSGRGGLGG  120
QGAGAAAAAG GAGQGGYGGL GSQGTSGRGG LGGQGAGAAA AAGGAGQGGY GGLGSQGTSG  180
RGGLGGQGAG AAAAAGGAGQ GGYGGLGSQG TSGRGGLGGQ GAGAAAAAGG AGQGGYGGLG  240
SQGTSGRGGL GGQGAGAAAA AGGAGQGGYG GLGSQGTSGR GGLGGQGAGA AAAAGGAGQG  300
GYGGLGSQGT SGRGGLGGQG AGAAAAAGGA GQGGYGGLGS QGTSGRGGLG GQGAGAAAAA  360
GGAGQGGYGG LGSQGTSGRG GLGGQGAGAA AAAGGAGQGG YGGLGSQGTS GRGGLGGQGA  420
GAAAAAGGAG QGGYGGLGSQ GTSGRGGLGG QGAGAAAAAG GAGQGGYGGL GSQGTSGRGG  480
LGGQGAGAAA AAGGAGQGGY GGLGSQGTSG RGGLGGQGAG AAAAAGGAGQ GGYGGLGSQG  540
TSSSKKSGSY SGSKGSKRRI L                                            561
```

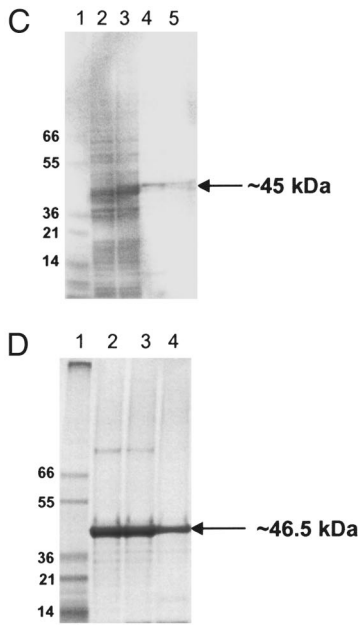

Fig. 2. Expression and purification of spider silk fusion proteins. Amino acid sequences and gel electrophoresis of the bioengineered spider silk fusion proteins CRGD15mer+R5 (*A*) and 15mer+R5 (*B*). Underlined is the representative monomeric repeat unit selected and used in the design of the recombinant proteins based on the consensus sequence of spidroin 1 (Masp1) native sequence of *N. clavipes* (GenBank accession no. P19837). (*C*) Gel electrophoresis of 15mer+R5: lane 1, ladder; lane 2, flow-through; lane 3, wash 1; lane 4, elution 1; lane 5, elution 2. (*D*) Gel electrophoresis of CRGD15mer+R5: lanes 1, ladder; lane 2, elution 1; lane 3, elution 2; lane 4, elution 3 treated with 10 mM DTT.

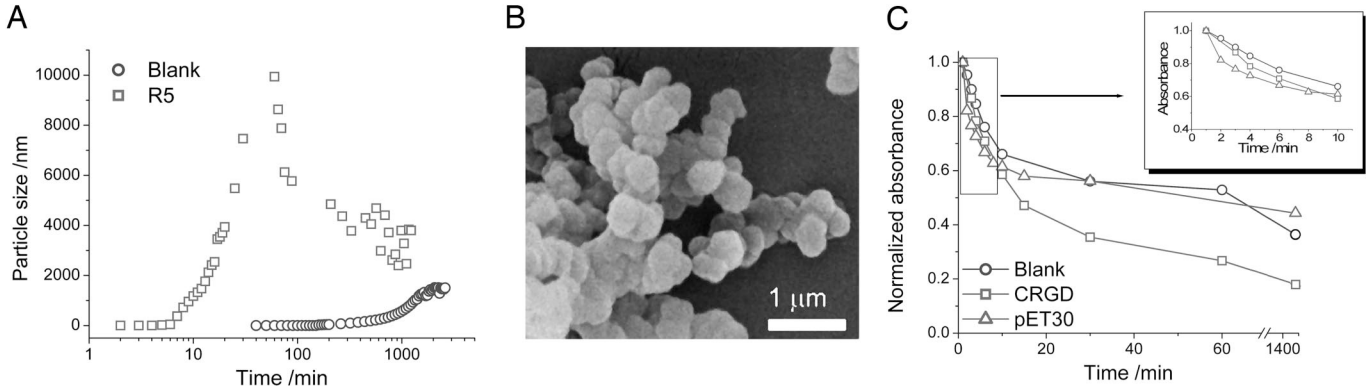

Fig. 3. Effect of R5 peptide and fusion proteins on silicification. (*A*) Dynamic light scattering data for silica obtained from experiments performed in the presence of R5 alone. (*B*) Typical SEM of silica formed in the presence of 1 silicon:1 nitrogen-containing amino acid in R5 at pH 7.0 from aqueous solution. The ratio of silicon to nitrogen containing amino acid side chains in R5 was kept constant at 1:1 to allow comparison with our previous studies using simple amino acids, peptides, and small amines (44, 45). (*C*) Normalized absorbance from soluble silicon released from a 30 mM aqueous solution of a silicon catecholato complex in the presence and absence of fusion proteins (silk+R5) over 24 h at pH adjusted to ≈6.8 as described previously (44, 45).

relationships. To this end, a range of material morphologies and properties can now be generated through control of solution conditions, concentration, and additives, such that electrospun fibers (30, 31), films (32), porous matrices (33, 34), and hydrogels (35) can be generated under controlled conditions from these silk proteins that otherwise form into fibers only during processing in nature. The remarkable materials properties of these proteins prompt interest in their functionalization for enhancement in properties. For example, we have reported the successful chemical decoration of silk-based biomaterials with cell binding domains (36) and with cytokines such as bone morphogenetic protein 2 to enhance bone tissue formation (37).

The fusion proteins used in this study were generated by using a genetically engineered variant of a synthetic spider silk gene with the R5-encoding gene (Fig. 2) by using cloning strategies previously described (38–40). The amino acid sequences of the two spider dragline silk fusion proteins with silicification-inducing domains, with (type 1) and without (type 2) a CRGD cell-binding motif, are shown in Fig. 2.

Results and Discussion

When the R5 peptide was used alone at a ratio of one silicon to one amine from the side chains of R5 there was little difference in the rate of removal of soluble silicon species from solution (data not shown), suggesting little catalytic effect on the early stages of silicic acid polymerization. However, rapid precipitation of silica–peptide composites from the reaction media was observed (Fig. 3*A*), consistent with previous studies (11, 13, 15). The precipitate formed showed that the silica formed is highly "dense" (surface area with and without R5 was 6.4 and 600 m^2/g, respectively). Upon calcination and removal of the organic phase from the silica–protein composite, the surface area increased to 520 m^2/g, implying occlusion of the peptide in the silica particles. The particles were found to be spheres of size ≈1 μm (Fig. 3*B*). The role of R5 seems to be in aggregation and scaffolding rather than catalysis.

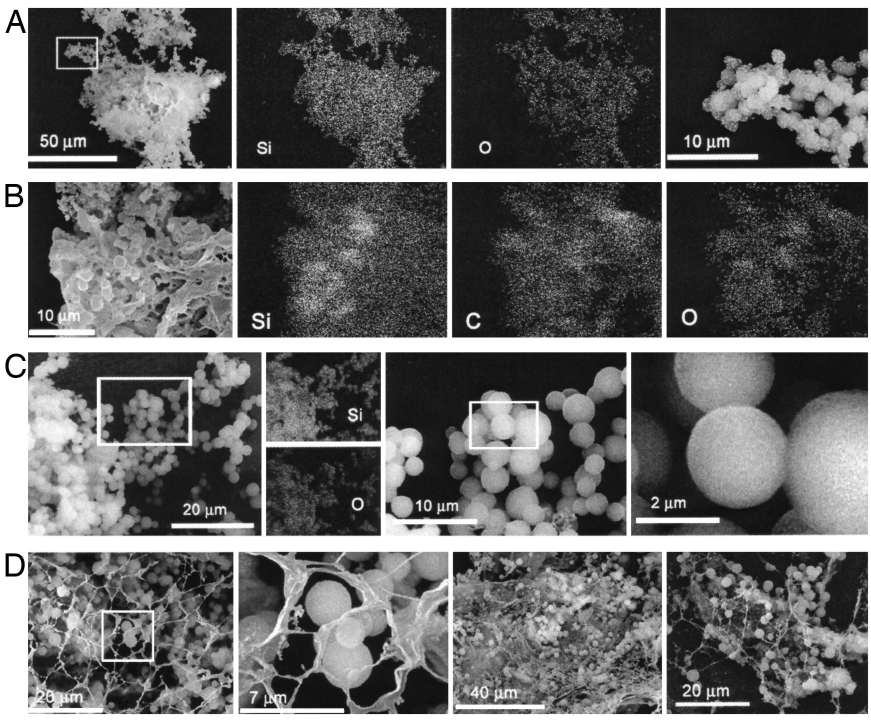

Fig. 4. Morphological and elemental analyses of nanocomposites. SEM images of silica composite materials generated from an aqueous-based dipotassium silicon triscatecholate complex in the presence of chimera CRGD15mer+R5 (*A* and *B*) and chimera 15mer+R5 (*C* and *D*). Areas highlighted by rectangles are presented at higher magnification in the same rows. In *A*–*C* elemental maps are shown for silicon (Si), oxygen (O), and/or carbon (C).

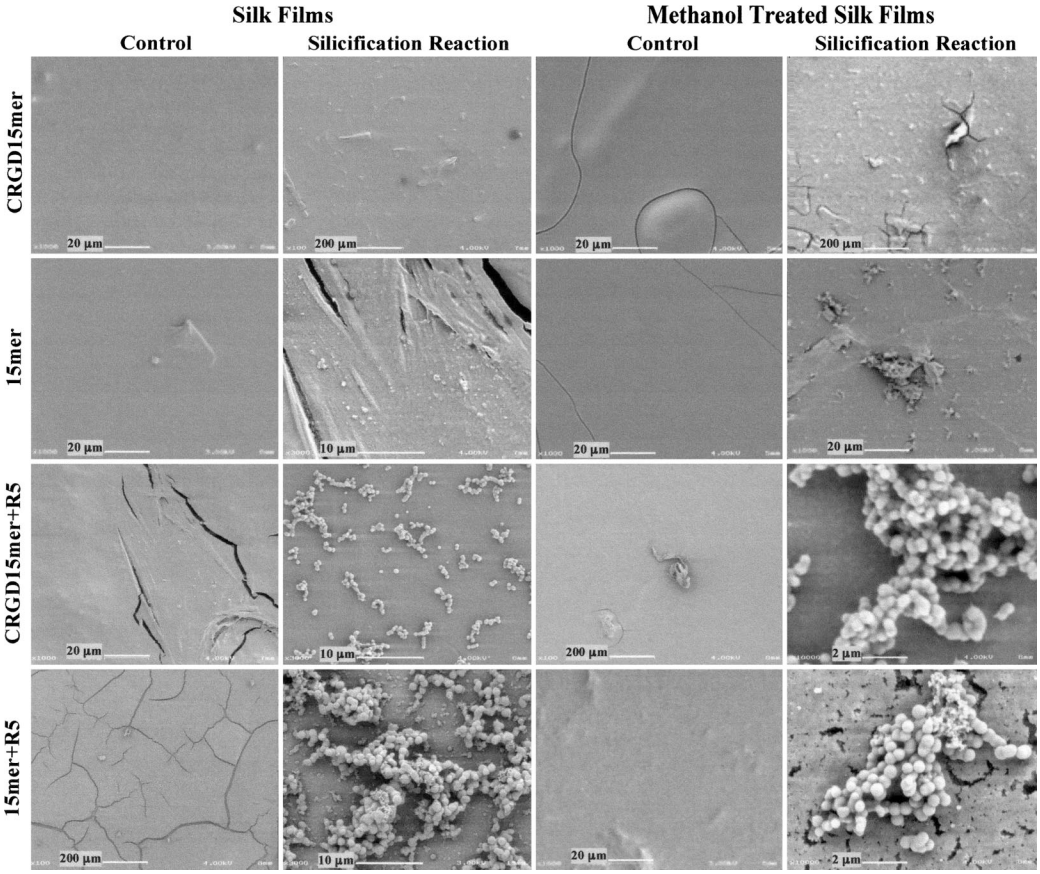

Fig. 5. SEM images of untreated and methanol-treated silk films formed from four different genetically engineered silk proteins: CRGD15mer, 15mer, CRGD15mer+R5, and 15mer+R5. Images of the control films and the films that underwent silicification reactions are shown.

Furthermore, the silk+R5 fusion proteins were introduced into the silica polymerization experiments, data were obtained on kinetics of silicic acid polymerization, and morphology and porosity of silica precipitated. Even at low levels of fusion protein (≈135 silicon:1 R5 from fusion proteins, i.e., ≈22 silicon:1 amine groups from amino acid side chains of R5) there was an effect on the rate of removal of silicic acid from solution and on the nature of the silica phase formed (Fig. 3*C*). Electron microscopy images of the precipitated silica showed networks of spheres of approximately >1 μm in diameter. These particles were similar in appearance to the silica produced in the presence of R5 alone where the silicon:amine from R5 was equal to one (Fig. 4). The elemental mapping of the samples (Fig. 4) revealed that the product contained silicon and oxygen arising from silica. The high amounts of carbon (Fig. 4*B*) can be attributed to occluded protein. From the scanning electron microscopy (SEM) data (Fig. 4*D*) it can be seen that, even without using any special assembly techniques, self-assembly of the silk chimera was evident in the presence of the silica structures. Thermal analysis was carried out on the samples, and the data suggest that ≈90% of the material was protein and the remaining 10% was silica. Nitrogen adsorption analysis of the composite samples indicated pore radii of the silica <10 Å and very low surface areas (≈10 m^2/g) when compared with blank samples (≈35 Å and ≈600 m^2/g, respectively).

To exploit the self-assembling properties of silk in developing silk–silica nanocomposites, experiments were performed with tetramethoxysilane as the precursor. Four genetically engineered variants of the spider silk protein [two controls (one with and one without RGD but both without R5) and two chimeric versions of the controls with R5] were cast into films that were left untreated or were treated with methanol to induce a structural transition to β-sheets at the surface to decrease film solubility in aqueous buffer. Silicification reactions were performed on the films yielding spherical silica structures with diameters ranging from ≈0.5 to 2.0 μm only when the silica-precipitating domain, R5 peptide, was fused to the C terminus of the silk proteins (Fig. 5). The silk proteins that did not contain R5 (CRGD15mer and 15mer) did not yield significant changes in surface morphology of the films upon exposure to the silicification reactions.

Fusion proteins were assembled into fibers by electrospinning (Fig. 6). SEM images of the electrospun fibers formed from the chimeric proteins (Fig. 6*Ai*), and the morphological characteristics observed when the fibers were treated with methanol were similar to those we observed previously for electrospun silk fibroin with polyethylene oxide (31). Upon silicification on electrospun mats formed from the chimeric protein CRGD15mer+R5 without methanol treatment, similar spherical silica structures were observed as in the reactions on the cast films (Fig. 6*Aii*). However, the dimensions of the silica spheres were slightly smaller, ranging from 200 to 400 nm (Fig. 6*Aii*). When the electrospun fibers consisting of the chimera CRGD15mer+R5 were not treated with methanol, the fibers fused together on the surface (Fig. 6*Aii*). Without the β-sheet inducing methanol treatment, the fibers are prone to partially solubilize on the surface, yielding fused fibers or a thin film on which the mineralization reaction takes place. However, upon treatment of the chimera CRGD15mer+R5 electrospun mats with methanol before silicification, the fibers fused to a much lesser extent at the surface as expected (31), compared with fibers that were not treated with methanol, and silica nanospheres were either sparingly observed or not observed at all (data not shown). When the chimera CRGD15mer+R5 was electrospun during the silica polymerization process (concurrent processing), silica deposition

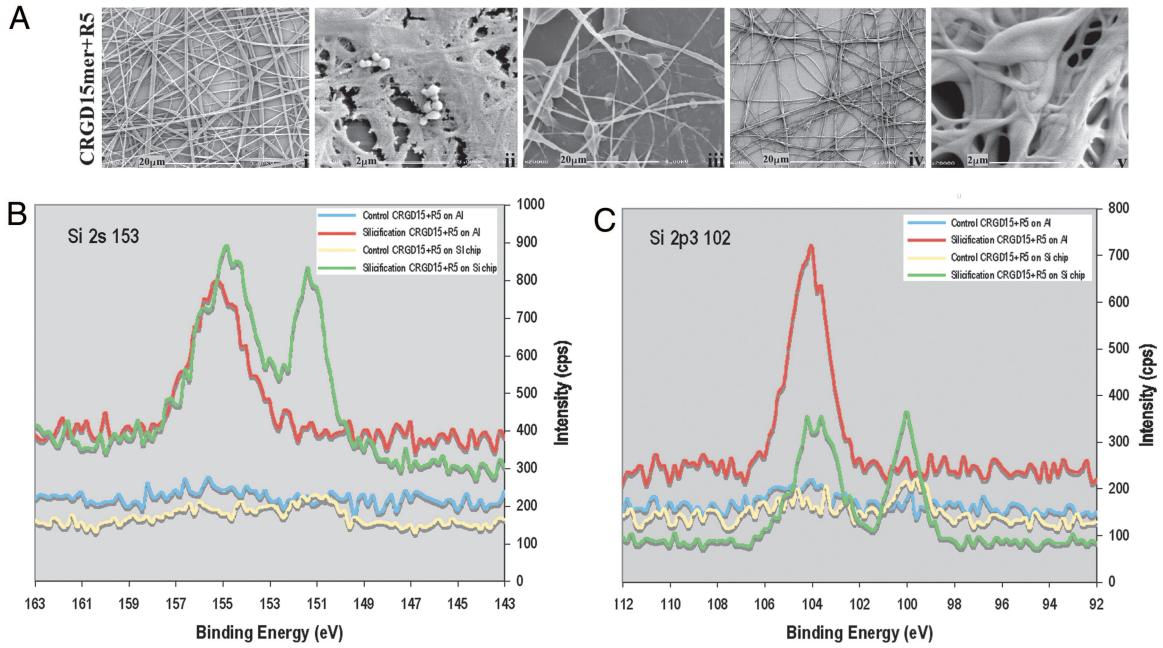

Fig. 6. Morphological characterization and elemental analysis of silica deposition on eletrospun fibers. (*A*) SEM images of untreated and treated electrospun CRGD15mer+R5 silk fibers before, during, and after silicification reactions. (*B* and *C*) X-ray photoelectron spectroscopy analysis of CRGD15mer+R5 and silicified CRGD15mer+R5 on Al foil and on silicon chip at the characteristic binding energies of 153 eV (*B*) and 102 eV (*C*) for electrons found in the 2s and 2p3 electron shells of the silicon atom, respectively.

was induced in and on the fibers, and elliptically shaped silica particles fused to the fibers were observed (Fig. 6*A iii--v*). The individual fibers appeared sticky and fused to each other to a greater extent, and silica deposition around the fibers provided a nonuniform coating instead of the usual heterogeneous distribution of silica nanospheres (Fig. 6*A iii--v*). X-ray photoelectron spectroscopy analysis of the resulting fibers confirmed the presence of elemental silicon (Fig. 6 *B* and *C*). Thus, the concurrent processing approach, fiber spinning and silicification reactions, resulted in a different morphology of the silica in terms of location within the fibers and shape, compared with the silicification reactions conducted after electrospinning.

The design and use of novel chimeric fusion proteins containing silk and silica-forming domains in the synthesis of new silk–silica nanocomposites have been demonstrated. The properties of silk have been exploited to generate self-assembled composites in the form of films and fibers as examples to illustrate the diversity of processing options with this approach. Changes in processing conditions altered the size distribution as well as the morphology of the composites such that control of process details will provide control of the mineral phase and thus composite properties. The protein biomaterial self-assembling nanodomains used in these designs are genetically tailorable in terms of size, chemistry, and morphology, such that this approach offers a new platform for *in situ* silica formation with unprecedented control in composite materials design and properties. The silica-forming domain is also tailorable in terms of sequence chemistry to influence reaction kinetics and materials features. The silica-forming domains can also be replaced with alternative fusions and thereby be used to form other inorganic phases (e.g., hydroxyapatite, titanium dioxide, and germania); thus, the versatility and opportunities that can be explored with this chimeric biomimetic protein design strategy are expansive. This approach to nanoscale material composite systems engineering, we believe, will generate new families of biomaterials that can be either preassembled *in vitro* or organized (self-assembled) *in vivo*. The novelty and potential utility of the strategy described are further extended by the molecular-level connections between the organic (silk) and inorganic (silica) phases because of the chimeric design of the protein chains, as well as because of the all aqueous and ambient conditions under which materials formation is conducted. Specifically, the all-aqueous conditions offer future options to consider *in situ* reactions in tissue-compatible compartments *in vivo*; the domain sizes of the silica particles formed are in a size scale that makes them suitable candidates for *in vivo* needs as glassy biomaterials, compared with larger bulk silica or bioactive glass systems usually used as bioactive composites (41, 42). The ability to direct the silica-forming reactions to material interfaces is a plus in regulating materials morphology and thus function. This attribute is derived from the water-based processing and the resulting hydrophobic–hydrophilic partitioning of the hydrophobic silk protein component of the chimera and the hydrophilic R5 component.

Materials and Methods

Design and Expression of Recombinant Spider Silk Protein. One repeat was designed and constructed for cloning by using synthetic oligonucleotides and then amplified by using PCR. The 15mer encoding the repeat was cloned through the transfer of cloned inserts between two shuttle vectors based on pUC19 and pCR-Script (39, 40) (Stratagene). The cloning of CRGD15mer recombinant protein was performed in a similar manner. Oligonucleotides for the R5 peptide were designed with EcoRI (gaattc) and NotI (gcggccgc) restriction sites at the 5′ and 3′ ends, respectively, and then ligated directly into the EcoRI and NotI restriction sites of pET-30a(+) vector (Novagen) next to the 15mer clone (Fig. 7, which is published as supporting information on the PNAS web site). The constructs pET-30a(+)-15mer+R5 and pET-21a(+)-CRGD15mer+R5 were transformed into the *Escherichia coli* host strain RY-3041, a mutant strain defective in the expression of SlyD protein, for protein expression (38, 43). The resulting proteins were finally purified under denaturing conditions using an Ni-NTA resin (Qiagen, Valencia, CA), which allows for the specific binding of the 6×His fusion tag at the C terminus of the proteins. The purified

proteins were then identified by using SDS/PAGE (Invitrogen) (Fig. 2 *C* and *D*).

Preparation of Silica Samples. To establish baseline model reaction conditions for silica polymerization in the presence of R5, two different silica precursors were used, tetramethoxysilane and a silicon–catecholate complex (44, 45). Typically, for silica precipitation with or without the presence of proteins, 30 mM silicic acid was used, unless otherwise stated. Silica synthesis was carried out as described previously (11, 12, 14, 15, 44, 45). The reaction mixture was allowed to condense for a desired period while aliquots at known time were taken for molybdosilicate kinetic assay (44). Silica samples were isolated by centrifugation, washed, and lyophilized for SEM and nitrogen adsorption analyses. Nitrogen gas adsorption/desorption analysis was carried out by using a Quantachrome Nova3200e surface area and pore size analyzer. Surface areas were determined through the Brunauer–Emmett–Teller method (46), and pore radii were determined by the Barrett–Joiner–Halenda method (47) using the desorption branch of the isotherm. The entrapped organic material in silica was removed by calcination of samples at 650°C in air. Samples for SEM were prepared by dispersing the lyophilized powder on sample holders containing double-sided sticky carbon tape and gold coated under argon plasma.

Preparation of Silk Films. The lyophilized fusion proteins were dissolved in hexafluoroisopropanol at a concentration of 2.5% wt/vol at 4°C. A total of 100 μl of the protein–hexafluoroisopropanol solution was pipetted directly onto chemically inert silicon chips placed at the bottom of 24-well culture plates and allowed to air-dry. The silk films were then left untreated or were treated with a 90% vol/vol methanol/water mixture to induce β-sheet formation on the films surfaces and therefore prevent resolubilization of the films in aqueous solutions.

Silicification Reactions on Cast Films. A total of 200 μl of 100 mM phosphate buffer at pH 5.5 was added to cover the air-dried silk films formed on the silicon chips and were left to incubate for 30 min at room temperature. A total of 20 μl of 1 M tetramethoxysilane hydrolyzed in 1 mM hydrochloric acid was then added for the silicification reaction to take place, and the reaction was left to incubate for ≈10 min (37). The films were then washed with 18.2 MΩ water three times and left to dry overnight in the fume hood. The morphologies of the exposed surface of these processed silk films with silica deposition were then analyzed by using a LEO 982 Scanning Electron Microscope (Harvard University Center for Nanoscale Systems, Cambridge, MA).

Electrospinning of Silk Fibers and Silicification Reactions. Fibers of the recombinant spider silk proteins were electrospun directly onto silicon chips placed on the Al foil-covered receiving plate by using a 2% wt/vol solution of recombinant spider silk in hexafluoroisopropanol as previously described (31). The concentrated silk solution was infused at the rate of 0.01 ml/min at 15–20 kV. Some of the electrospun fibers were then treated with 90% vol/vol methanol in water to induce β-sheet formation by incubation for 10 min and were finally allowed to air-dry.

The same procedure as for the cast films was used to perform the silicification reactions on both methanol-treated and nonmethanol-treated electrospun fiber mats. Furthermore, silicification reactions were performed during electrospinning by injecting the silicic acid solution mixed with phosphate buffer at the same rate and time as the concentrated silk solution.

SEM was used to perform morphological characterization of the electrospun fibers, with and without methanol treatment and silicification reactions, by using a Leo 982 Field Emission Scanning Electron Microscope (Harvard University Center for Nanoscale Systems). Furthermore, elemental analysis of the unreacted and reacted samples was performed by using an x-ray photoelectron spectrometer equipped with an Al K_a radiation source and four available spot sizes ranging from 150 to 1,000 mm (Harvard University Center for Nanoscale Systems).

We thank the National Institutes of Health (Grants EB00252 and EB003210), the U.S. Air Force Office of Scientific Research (Grants FA9550041 and F49620-03-1-0099), and the European Commission (SILIBIOTEC Project QLK3-CT-2002-01967) for their financial support.

1. Heuer, A. H., Fink, D. J., Laraia, V. J., Arias, J. L., Calvert, P. D., Kendall, K., Messing, G. L., Blackwell, J., Rieke, P. C., Thompson, D. H., *et al*. (1992) *Science* **255,** 1098–1105.
2. Boskey, A. L. (1998) *J. Cell. Biochem. Suppl.* **30–31,** 83–91.
3. Li, C., Vepari, C., Jin, H. J., Kim, H. J. & Kaplan, D. L. (2006) *Biomaterials* **27,** 3115–3124.
4. Wilt, F. H. (2005) *Dev. Biol.* **280,** 15–25.
5. Muller, W. E. G. (2003) *Silicon Biomineralization* (Springer, Berlin).
6. Simpson, T. L. & Volcani, B. E. (1981) *Silicon and Siliceous Structures in Biological Systems* (Springer, New York).
7. Wong Po Foo, C., Huang, J. & Kaplan, D. L. (2004) *Trends Biotechnol.* **22,** 577–585.
8. Perry, C. C. & Keeling-Tucker, T. (2000) *J. Biol. Inorg. Chem.* **5,** 537–550.
9. Voronkov, M. G. (1977) *Silicon and Life* (Zinatne, Vilnius, Lithuania).
10. Patwardhan, S. V., Clarson, S. J. & Perry, C. C. (2005) *Chem. Commun.* **9,** 1113–1121.
11. Sumper, M. & Kroger, N. (2004) *J. Mater. Chem.* **14,** 2059–2065.
12. Brott, L. L., Pikas, D. J., Naik, R. R., Kirkpatrick, S. M., Tomlin, D. W., Whitlock, P. W., Clarson, S. J. & Stone, M. O. (2001) *Nature* **413,** 291–293.
13. Naik, R. R., Whitlock, P. W., Rodriguez, F., Brott, L. L., Glawe, D. D., Clarson, S. J. & Stone, M. O. (2003) *Chem. Commun.* 238–239.
14. Patwardhan, S. V. (2003) Ph.D. dissertation (Univ. of Cincinnati, Cincinnati).
15. Whitlock, P. W. (2005) Ph.D. dissertation (Univ. of Cincinnati, Cincinnati).
16. Knecht, M. R. & Wright, D. W. (2003) *Chem. Commun.* 3038–3039.
17. Albarran, B., To, R. & Stayton, P. S. (2005) *Protein Eng. Des. Selection* **18,** 147–152.
18. Asai, T., Trinh, R., Ng, P. P., Penichet, M. L., Wims, L. A. & Morrison, S. L. (2005) *Biomol. Eng.* **21,** 145–155.
19. Icke, C., Schlott, B., Ohlenschlager, O., Hartmann, M., Guhrs, K. H. & Glusa, E. (2002) *Mol. Pharmacol.* **62,** 203–209.
20. Park, E., Starzyk, R. M., McGrath, J. P., Lee, T., George, J., Schutz, A. J., Lynch, P. & Putney, S. D. (1998) *J. Drug Targeting* **6,** 53–64.
21. Dubrovsky, T., Tronin, A., Dubrovskaya, S., Guryev, O. & Nicolini, C. (1996) *Thin Solid Films* **285,** 698–702.
22. Frey, W., Meyer, D. E. & Chilkoti, A. (2003) *Adv. Mater.* **15,** 248-251.
23. Medintz, I. L., Uyeda, H. T., Goldman, E. R. & Mattoussi, H. (2005) *Nat. Mater.* **4,** 435–446.
24. Padilla, J. E., Colovos, C. & Yeates, T. O. (2001) *Proc. Natl. Acad Sci. U.S.A.* **98,** 2217–2221.
25. Paternolli, C., Ghisellini, P. & Nicolini, C. (2002) *Mater. Sci. Eng. C* **22,** 155–159.
26. Sleytr, U. B., Schuster, B. & Pum, D. (2003) *IEEE Eng. Med. Biol. Mag.* **22,** 140–150.
27. Slocik, J. M., Naik, R. R., Stone, M. O. & Wright, D. W. (2005) *J. Mater. Chem.* **15,** 749–753.
28. Cunniff, P. M., Fossey, S. A., Auerbach, M. A. & Song, J. W. (1994) in *Silk Polymers* (Am. Chem. Soc., Washington, DC), Vol. 544, pp. 234–251.
29. Gosline, J. M., Demont, M. E. & Denny, M. W. (1986) *Endeavour* **10,** 37–43.
30. Wong Po Foo, C., Bini, E., Hensman, J., Knight, D. P., Lewis, R. V. & Kaplan, D. L. (2006) *Appl. Phys. A* **82,** 223–233.
31. Jin, H. J., Fridrikh, S. V., Rutledge, G. C. & Kaplan, D. L. (2002) *Biomacromolecules* **3,** 1233–1239.
32. Jin, H. J., Park, J., Valluzzi, R., Cebe, P. & Kaplan, D. L. (2004) *Biomacromolecules* **5,** 711–717.
33. Kim, U. J., Park, J., Kim, H. J., Wada, M. & Kaplan, D. L. (2005) *Biomaterials* **26,** 2775–2785.
34. Nazarov, R., Jin, H. J. & Kaplan, D. L. (2004) *Biomacromolecules* **5,** 718–726.
35. Kim, U. J., Park, J. Y., Li, C. M., Jin, H. J., Valluzzi, R. & Kaplan, D. L. (2004) *Biomacromolecules* **5,** 786–792.
36. Sofia, S., McCarthy, M. B., Gronowicz, G. & Kaplan, D. L. (2001) *J. Biomed. Mater. Res.* **54,** 139–148.
37. Karageorgiou, V., Meinel, L., Hofmann, S., Malhotra, A., Volloch, V. & Kaplan, D. (2004) *J. Biomed. Mater. Res.* **71A,** 528–537.
38. Huang, J., Valluzzi, R., Bini, E., Vernaglia, B. & Kaplan, D. L. (2003) *J. Biol. Chem.* **278,** 46117–46123.
39. Prince, J. T., McGrath, K. P., Digirolamo, C. M. & Kaplan, D. L. (1995) *Biochemistry* **34,** 10879–10885.
40. Winkler, S., Wilson, D. & Kaplan, D. L. (2000) *Biochemistry* **39,** 12739–12746.
41. Boccaccini, A. R., Notingher, I., Maquet, V. & Jerome, R. (2003) *J. Mater. Sci. Mater. Med.* **14,** 443–450.
42. Wang, M. (2003) *Biomaterials* **24,** 2133–2151.
43. Yan, S. Z., Beeler, J. A., Chen, Y., Shelton, R. K. & Tang, W. J. (2001) *J. Biol. Chem.* **276,** 8500–8506.
44. Belton, D., Paine, G., Patwardhan, S. V. & Perry, C. C. (2004) *J. Mater. Chem.* **14,** 2231–2241.
45. Belton, D., Patwardhan, S. V. & Perry, C. C. (2005) *Chem. Commun.*, 3475–3477.
46. Brunauer, S., Emmett, P. H. & Teller, E. (1938) *J. Am. Chem. Soc.* **60,** 309–319.
47. Barrett, E. P., Joyner, L. G. & Halenda, P. P. (1951) *J. Am. Chem. Soc.* **73,** 373–380.